

Attractive Electromagnetic Casimir Stress on a Spherical Dielectric Shell

N. Graham,¹ M. Quandt,² and H. Weigel³

¹*Department of Physics, Middlebury College Middlebury, VT 05753, USA*

²*Institute for Theoretical Physics, University of Tübingen, D-72076 Tübingen, Germany*

³*Physics Department, Stellenbosch University, Matieland 7602, South Africa*

Based on calculations involving an idealized boundary condition, it has long been assumed that the stress on a spherical conducting shell is repulsive. We use the more realistic case of a Drude dielectric to show that the stress is attractive, matching the generic behavior of Casimir forces in electromagnetism. We trace the discrepancy between these two cases to interactions between the electromagnetic quantum fluctuations and the dielectric material.

PACS numbers: 03.50.De, 03.65.Nk, 11.80.Et, 11.80.Gw

After discovering the quantum-mechanical force between uncharged conductors that bears his name, Casimir proposed using this force to model the electron as a uniformly charged spherical shell whose size is fixed by balancing its attractive Casimir stress against its electrostatic repulsion [1]. Subsequent calculations [2, 3], however, found a repulsive rather than attractive stress in this geometry, and in any case quantum electrodynamics provides a fuller description of the electron. Since then, this result has been extrapolated outside the realm of fundamental physics, with the result that the existence of a repulsive Casimir stress on a conducting sphere has been taken as a standard result in the field, even though it is very much at odds with the attractive *force* between two hemispheres [4] and is not robust against the infinitesimal deformation or nonzero thickness of the spherical shell.

In this Letter we argue that, when applied to a mesoscopic conducting shell, Casimir's original picture of an attractive force was indeed correct. At the center of the difficulty in computing Casimir stresses are the divergences — more precisely, the dependences on the short-distance cutoff — inherent in these calculations. While a fundamental theory of the electron can postulate any model for these short-distance effects, a calculation relevant to mesoscopic materials does not have this freedom. Instead, we employ the standard Drude model for metals (though the simpler plasma model yields similar results). The field theory cutoff must be imposed at distances shorter than any other scale in the problem; in particular, the cutoff must be at scales shorter than the plasma wavelength, at which the material no longer acts as a perfect conductor. As a result, it is essential that these two limits are taken in the correct order, which implies that fluctuations at the scale of the cutoff should always see the material as transparent.

While we will use a generic dielectric to model the shell material, our results agree qualitatively with results obtained from more specific models, such as a carbon nanostructure [5] or a “fish-eye” medium [6]. Our findings are also in agreement with the work of Deutsch and Candelas [7, 8], who showed that divergences in Casimir

stresses arise from surface counterterms [9] that cannot be removed by renormalization, and with explicit calculations in scalar models [10–12]. We note that the Casimir energy of an idealized boundary can be of interest for the mathematical “Weyl problem” of the relationship between eigenvalue spectra and geometry [13, 14]. This approach draws on classic results relating the shape of a boundary to the density of scattering states [15, 16], but does not make direct contact with a physically measurable stress.

We model the shell as a space- and frequency-dependent Drude dielectric,

$$\epsilon_k(r) = 1 + \frac{(2\pi)^2}{-(\lambda_p k)^2 + \frac{\pi}{\sigma_p} \sqrt{-k^2}} p(r) \quad (1)$$

where $p(r)$ is a spherically symmetric profile function that goes to zero for $r \rightarrow \infty$, λ_p is the plasma wavelength, σ_p is the conductivity, and there is no free charge. We decompose the quantum fluctuations by frequency $\omega = ck$ and work in units where $\hbar = c = 1$. Because we maintain spherical symmetry and parity, the transverse electric (TE) and transverse magnetic (TM) modes decouple. As a result, we can use the method of Ref. [17] to reduce each channel to a scalar scattering problem. For the TE mode, we parameterize the electric field as

$$\mathbf{E}_k(\mathbf{r}) = k \nabla \times [\varphi_k(\mathbf{r}) \mathbf{r}] = -k \mathbf{r} \times \nabla \varphi_k(\mathbf{r}), \quad (2)$$

which obeys

$$\nabla \cdot (\epsilon_k(r) \mathbf{E}_k(\mathbf{r})) = \nabla \cdot [k \nabla \times (\epsilon_k(r) \varphi_k(\mathbf{r}) \mathbf{r})] = 0 \quad (3)$$

and solves the Maxwell equation

$$\nabla \times \nabla \times \mathbf{E}_k(\mathbf{r}) = k^2 \epsilon_k(r) \mathbf{E}_k(\mathbf{r}) \quad (4)$$

if $-\nabla^2 \varphi_k(\mathbf{r}) = k^2 \epsilon_k(r) \varphi_k(\mathbf{r})$. We solve the latter equation using separation of variables

$$\varphi_{k,\ell m}(\mathbf{r}) = \frac{1}{\sqrt{\ell(\ell+1)}} Y_\ell^m(\theta, \phi) \frac{1}{r} f_{k,\ell}(r). \quad (5)$$

with $\ell = 1, 2, 3, \dots$ and

$$-f_{k,\ell}''(r) + \frac{\ell(\ell+1)}{r^2} f_{k,\ell}(r) - k^2 \epsilon_k(r) f_{k,\ell}(r) = 0. \quad (6)$$

Here, the prime denotes a derivative with respect to r .

For the TM mode, we take

$$\mathbf{B}_k(\mathbf{r}) = \frac{k}{i} \nabla \times [\phi_k(\mathbf{r})\mathbf{r}], \quad (7)$$

which obeys $\nabla \cdot \mathbf{B}_k(\mathbf{r}) = 0$. Then we have

$$\mathbf{E}_k(\mathbf{r}) = \frac{i}{k\epsilon_k(r)} \nabla \times \mathbf{B}_k(\mathbf{r}) = \frac{1}{\epsilon_k(r)} \nabla \times \nabla \times [\phi_k(\mathbf{r})\mathbf{r}], \quad (8)$$

which obeys $\nabla \cdot [\epsilon_k(r)\mathbf{E}_k(\mathbf{r})] = 0$. Again we use separation of variables to write the solution in the form

$$\phi_{k,\ell m}(\mathbf{r}) = \frac{\sqrt{\epsilon_k(r)}}{\sqrt{\ell(\ell+1)}} Y_\ell^m(\theta, \phi) \frac{1}{r} g_{k,\ell}(r). \quad (9)$$

The Maxwell equation $\nabla \times \mathbf{B}_k(\mathbf{r}) = -ik\epsilon_k(r)\mathbf{E}(\mathbf{r})$ then gives

$$k^2 g_{k,\ell}(r) = -g_{k,\ell}''(r) + \frac{\ell(\ell+1)}{r^2} g_{k,\ell}(r) + \left[k^2(1 - \epsilon_k(r)) + \frac{3\epsilon_k'(r)^2}{4\epsilon_k(r)^2} - \frac{\epsilon_k''(r)}{2\epsilon_k(r)} \right] g_{k,\ell}(r), \quad (10)$$

where in Eq. (9) we have introduced the scaling factor $\sqrt{\epsilon_k(r)}$ to ensure that the single-particle wave equation is Hermitian.

A single frequency mode contributes the energy density

$$\frac{1}{2} \epsilon_k(r) \mathbf{E}_k(\mathbf{r})^2 + \frac{1}{2} \mathbf{B}_k(\mathbf{r})^2.$$

Integration over space and use of the wave equation yields an expression for the total energy that takes the same form in both channels,

$$E = \int_0^\infty dk \sum_{\ell=1}^\infty (2\ell+1) \frac{k}{\pi} \int_0^\infty dr \left(\epsilon_k(r) |\psi_{k,\ell}(r)|^2 - |\psi_{k,\ell}^{(0)}(r)|^2 \right), \quad (11)$$

where ψ is the normalized regular solution for either f or g and we have summed over all fluctuating modes. In this expression, we have subtracted the energy in the absence of the shell using the corresponding free wavefunction $\psi_{k,\ell}^{(0)}(r)$.

To prepare to evaluate Eq. (11), we relate the radial integral to the scattering phase shift $\delta_\ell(k)$ through the density of states [11]. However, the presence of the $\epsilon_k(r)$ factor, which does not arise in ordinary potential scattering, introduces additional complications. In particular, the Jost function analysis of Ref. [11] now yields

$$\frac{1}{\pi} \frac{d\delta_\ell}{dk} = \frac{2}{\pi} \int_0^\infty dr \left[\frac{1}{2k} \frac{d}{dk} (k^2 - V_k(r)) |\psi_{k,\ell}(r)|^2 - |\psi_{k,\ell}^{(0)}(r)|^2 \right]. \quad (12)$$

The potential, $V_k(r)$, is $V_k^{\text{TE}}(r) = k^2(1 - \epsilon_k(r))$ and $V_k^{\text{TM}}(r) = k^2(1 - \epsilon_k(r)) + \frac{3\epsilon_k'(r)^2}{4\epsilon_k(r)^2} - \frac{\epsilon_k''(r)}{2\epsilon_k(r)}$ for the TE and TM channels, respectively. By contrast, for ordinary potential scattering, the factor of $\epsilon_k(r)$ would be absent from Eq. (11) and the potential would be k -independent, meaning that the r integrands in Eqs. (11) and (12) would coincide.

We can therefore write the unrenormalized energy as

$$E = \frac{1}{2\pi} \int_0^\infty k dk \sum_{\ell=1}^\infty (2\ell+1) \left[\frac{d\delta_\ell}{dk} + \int_0^\infty dr \left(\frac{1}{2k} \frac{dV_k(r)}{dk} + \epsilon_k(r) - 1 \right) |\psi_{k,\ell}(r)|^2 \right]. \quad (13)$$

For numerical calculation, this form is greatly preferable to Eq. (11), because it takes advantage of Eq. (12) to yield an expression in which the r integral has support only on a compact region; otherwise we would need to maintain the delicate cancellation between $|\psi_{k,\ell}(r)|^2$ and $|\psi_{k,\ell}^{(0)}(r)|^2$ as $r \rightarrow \infty$. It is the second term in brackets in the ℓ -summand in Eq. (13) that leads to a discrepancy between our results and previous calculations, such as Ref. [18].

The frequency integral is most conveniently calculated by the variable phase method of Ref. [11] on the imaginary axis $k = i\kappa$. In order to extend the integration to negative momenta, the factor k in Eq. (13) must be treated as $\sqrt{k^2}$. This term produces the branch cut on the imaginary axis along which we integrate. We parameterize (the analytic continuation of) the outgoing wave solution via spherical Riccati–Hankel functions as

$$i\kappa r h_\ell^{(1)}(i\kappa r) e^{\beta_{\kappa,\ell}(r)},$$

which gives $\delta_\ell(i\kappa) = -\lim_{r \rightarrow 0} \beta_{\kappa,\ell}(r)$, where $\beta_{\kappa,\ell}(r)$ obeys

$$-\beta_{\kappa,\ell}''(r) + 2\kappa \xi_\ell(\kappa r) \beta_{\kappa,\ell}'(r) - \beta_{\kappa,\ell}'(r)^2 + V_{i\kappa}(r) = 0 \quad (14)$$

with the boundary conditions $\lim_{r \rightarrow \infty} \beta_{\kappa,\ell}(r) = 0$ and $\lim_{r \rightarrow \infty} \beta_{\kappa,\ell}'(r) = 0$. Here $\xi_\ell(\kappa r)$ is given in terms of spherical Hankel functions as

$$\xi_\ell(z) = -\frac{\frac{d}{dz} \left(z h_\ell^{(1)}(iz) \right)}{z h_\ell^{(1)}(iz)}. \quad (15)$$

By also parameterizing the regular solution as

$$\psi_{i\kappa,\ell}(r) = \frac{h_{\kappa,\ell}(r)}{(2\ell+1)(-i\kappa)^\ell i\kappa r h_\ell^{(1)}(i\kappa r)}, \quad (16)$$

where $h_{\kappa,\ell}$ obeys

$$-h_{\kappa,\ell}''(r) - 2\kappa \frac{d}{dr} (\xi_\ell(\kappa r) h_{\kappa,\ell}(r)) + V_{i\kappa}(r) h_{\kappa,\ell}(r) = 0 \quad (17)$$

with $h_{\kappa,\ell}(0) = 0$ and $h'_{\kappa,\ell}(0) = 1$, we can express the norm squared of the wavefunction through the Green's function at coincident points as [11]

$$|\psi_{i\kappa,\ell}(r)|^2 = \kappa \frac{h_{\kappa,\ell}(r)e^{\beta_{\kappa,\ell}(r)}}{(2\ell+1)e^{\beta_{\kappa,\ell}(0)}}. \quad (18)$$

In the free case, it is given in terms of spherical Bessel and Hankel functions by

$$|\psi_{i\kappa,\ell}^{(0)}(r)|^2 = \kappa^2 r^2 j_\ell(i\kappa r) h_\ell^{(1)}(i\kappa r). \quad (19)$$

The energy given by Eq. (13) contains the usual divergences of quantum field theory and as a result depends on the ultraviolet cutoff. We must therefore renormalize the theory in a way that makes contact with physically measurable quantities. To do so requires that we focus attention on the region within the shell itself, since that is where the local counterterms are nonzero. We will require two renormalization steps: one for the leading quadratic divergence, and a second for the residual logarithmic divergence.

We follow the conventional prescription for the leading quadratic divergence, the “no tadpole” scheme, in which we subtract the leading Born approximation from the energy [10–12]. This quantity is local, that is, proportional to a simple integral over space of the potential.

To address the subleading logarithmic divergence, we adopt a specific scaling of the dielectric profile of the shell as a function of radius. In particular, we require that the integral $\int d^3\mathbf{r} V_k^{\text{TE}}(r)^2$ remain constant as we expand or contract the sphere radius. For a shell profile that is a perfect step function shape, constraining the integral of all powers of the potential would yield equivalent conditions. For a smooth profile function, we choose to fix the second power in particular because the logarithmic divergence makes this power the one to which our calculation is most sensitive. We use a profile function parameterized by a radius R and a steepness s ,

$$p(r) = \text{sech}[s(r - R)], \quad (20)$$

and then consider the difference between the cases $R = R_1$, $s = s_1$ and $R = R_2$, $s = s_2$ such that $\int_0^\infty r^2 \text{sech}^2[s_1(r - R_1)] dr = \int_0^\infty r^2 \text{sech}^2[s_2(r - R_2)] dr$. Our renormalized energy in each channel thus becomes

$$\begin{aligned} E_{\text{ren}} = & \int_0^\infty \frac{d\kappa}{2\pi} \Delta \left\{ \sum_{\ell=1}^\infty (2\ell+1) \left[\left(\beta_{\kappa,\ell}(0) - \beta_{\kappa,\ell}^{(1)}(0) \right) \right. \right. \\ & + \kappa^2 \int_0^\infty dr \left(-\frac{1}{2\kappa} \frac{dV_{i\kappa}(r)}{d\kappa} + \epsilon_{i\kappa}(r) - 1 \right) \\ & \left. \left. \times \left(\frac{h_{\kappa,\ell}(r)e^{\beta_{\kappa,\ell}(r)}}{(2\ell+1)e^{\beta_{\kappa,\ell}(0)}} - \kappa r^2 j_\ell(i\kappa r) h_\ell^{(1)}(i\kappa r) \right) \right] \right\}. \end{aligned} \quad (21)$$

where the first Born approximation $\beta_{\kappa,\ell}^{(1)}(r)$ is obtained by iteration of the differential equation (14) and $\Delta\{\dots\}$ indicates that we compute the difference between the cases

$R = R_2$, $s = s_2$ and $R = R_1$, $s = s_1$. The sum of this quantity over TE and TM channels then gives the total change in energy when expanding or contracting the shell. We call the term in Eq. (21) that does not (explicitly) involve the radial integral the *traditional* contribution, since it is the analog of a calculation that is based on the change of the density of states measured by the momentum derivative of the phase shift. We call the remaining term, which involves the radial integral, the *additional* contribution.

For imaginary momentum $k = i\kappa$ the dielectric function becomes real, as do the potentials, $V_{i\kappa}(r)$, in the wave equations. Rotating to the imaginary momentum axis has the further advantage that it allows us to change the order of angular momentum sums and linear momentum integration [19]. We perform the angular momentum sum first, cutting off the numerical computation at $\ell = \ell_{\text{max}}$ for the sum over angular momentum channels and $\kappa = \kappa_{\text{max}}$ for the subsequent (imaginary) momentum integral. For $\kappa > \kappa_{\text{max}}$ we fit a power law to the integrand and use that fit to estimate the contributions from large momenta. This procedure requires (i) that κ_{max} is large enough to be in the asymptotic regime and (ii) that the angular momentum sum up to ℓ_{max} has converged at κ_{max} . The convergence condition on the angular momentum sum is conditional: the larger κ , the larger we need to take ℓ_{max} . The condition on κ_{max} is not very severe, since $\kappa_{\text{max}} \sim 2.5s$ turns out to be sufficient. However, the angular momentum sum converges slowly and we need to take ℓ_{max} as big as 2000. Practically, these conditions can be met for the traditional contribution with moderate numerical computation, but the additional contribution is significantly more costly. For that reason we compute the additional contribution for several choices of $\ell_{\text{max}} \sim 1000$ and find the $\ell_{\text{max}} \rightarrow \infty$ result by extrapolation. It turns out that the contribution from this extrapolation is of similar magnitude in the TE and TM channels. But since the former is much smaller than the latter overall, the relative effect of the extrapolation is sizable in the TE channel but small in the TM channel.

A further complication arises because we require the Hankel functions numerically for any order and any argument. Standard algorithms [20] are not appropriate for very large order and very small arguments. To bypass this obstacle, we use those algorithms only to find $\xi_\ell(z)$ for $z \rightarrow \infty$ as a boundary value, and then solve the non-linear first order differential equation

$$\frac{d\xi_\ell(z)}{dz} = \xi_\ell^2(z) - 1 - \frac{\ell(\ell+1)}{z^2} \quad (22)$$

to determine the logarithmic derivative of the spherical Riccati–Hankel function for real z . Similarly, we do not use standard algorithms to find the free Green's function, but rather supplement the set of differential equations (17) by the case $V_{i\kappa}(r) \equiv 0$, which yields

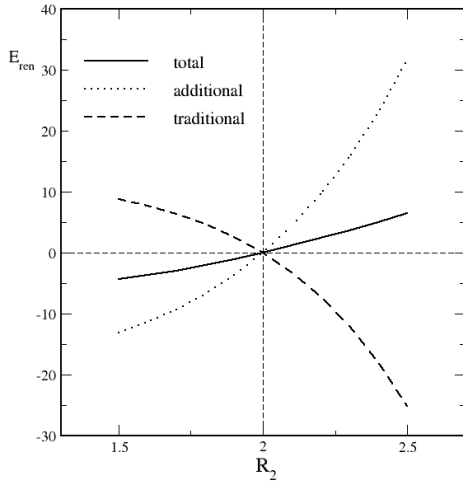


FIG. 1: Difference in renormalized energy between shells of radii R_2 and R_1 , as a function of R_2 for $R_1 = 2$.

$h_{\kappa,\ell}^{(0)}(r)$ with $|\psi_{i\kappa,\ell}^{(0)}|^2 = \frac{\kappa}{2\ell+1} h_{\kappa,\ell}^{(0)}(r)$. The numerical results presented here are based on FORTRAN codes. Those programs have also been tested against MATHEMATICA codes for moderate ℓ_{\max} and κ_{\max} .

In order to make the numerical calculation tractable, we choose moderate values of the model and ansatz parameters, rather than attempting to closely model a physical metallic sphere. Our results, however, are representative of the generic behavior of the stress on a dielectric shell. We work in units where $\lambda_p = 2$ and assume, for simplicity, that $\sigma = \lambda_p$. We choose as our reference contribution a shell with $R_1 = 2$ and $s_1 = 4$ in these units.

In Figure 1, we see that the traditional contribution, *i.e.* the one solely based on the phase shift (or equivalently, the logarithm of the Jost function [18]), decreases with increasing radii which would indeed lead to a repulsive self-stress if it were the sole contribution. On the other hand, the additional contribution due to the energy dependence of the dielectric, which is localized at the shell and depends on its material properties, is attractive. In total, the contribution from the additional term overcomes the standard repulsion and we find the electromagnetic Casimir stress of a spherical dielectric shell to be attractive, in agreement with the generic behavior of electromagnetic Casimir forces.

Our result shows how the attractive Casimir stress on a dielectric shell arises from a term that is not captured by the idealized boundary condition calculation. The additional contribution clearly originates from the frequency dependence of the dielectric and therefore is a manifesta-

tion of material properties. Because the dominant contribution originates in terms in $V_k^{\text{TM}}(r)$ proportional to space derivatives of $\epsilon_k(r)$, this result nonetheless persists in any limit in which the dielectric approaches such a boundary. We expect this behavior to apply to other cases for which the ideal boundary suggests a repulsive stress, such as a rectangular box, again in agreement with the results from Casimir forces [21], although it is more difficult to formulate the numerical calculation in that case.

N. G. was supported in part by the National Science Foundation (NSF) through grant PHY-1213456. H. W. was supported by the National Research Foundation (NRF), Ref. No. IFR1202170025.

-
- [1] H. B. G. Casimir, *Physica* **XIX**, 846 (1953).
 - [2] T. H. Boyer, *Phys. Rev.* **174**, 1764 (1968).
 - [3] K. A. Milton, L. L. DeRaad Jr., and J. S. Schwinger, *Annals Phys.* **115**, 388 (1978).
 - [4] O. Kenneth and I. Klich, *Phys. Rev. Lett.* **97**, 160401 (2006).
 - [5] G. Barton, *J. Phys.* **A37**, 1011 (2001).
 - [6] U. Leonhardt and W. M. R. Simpson, *Phys. Rev.* **D84**, 081701 (2011).
 - [7] D. Deutsch and P. Candelas, *Phys. Rev.* **D20**, 3063 (1979).
 - [8] P. Candelas, *Annals Phys.* **143**, 241 (1982).
 - [9] K. Symanzik, *Nucl. Phys.* **B190**, 1 (1981).
 - [10] N. Graham, R. L. Jaffe, V. Khemani, M. Quandt, M. Scandurra, and H. Weigel, *Phys. Lett.* **B572**, 196 (2003).
 - [11] N. Graham, R. L. Jaffe, V. Khemani, M. Quandt, M. Scandurra, and H. Weigel, *Nucl. Phys.* **B645**, 49 (2002).
 - [12] N. Graham, R. L. Jaffe, V. Khemani, M. Quandt, O. Schröder, and H. Weigel, *Nucl. Phys.* **B677**, 379 (2004).
 - [13] E. K. Abalo, K. A. Milton, and L. Kaplan, *J. Phys.* **A45**, 425401 (2012).
 - [14] E. B. Kolomeisky, J. P. Straley, L. S. Langsjoen, and H. Zaidi, *J. Phys.* **A43**, 385402 (2010).
 - [15] R. Balian and C. Bloch, *Annals Phys.* **60**, 401 (1970).
 - [16] R. Balian and B. Duplantier, *Annals Phys.* **104**, 300 (1977).
 - [17] B. R. Johnson, *J. Opt. Soc. Am. A* **16**, 845 (1999).
 - [18] M. Bordag and N. Khusnutdinov, *Phys. Rev.* **D77**, 085026 (2008).
 - [19] O. Schröder, N. Graham, M. Quandt, and H. Weigel, *J. Phys.* **A41**, 164049 (2008).
 - [20] W. H. Press, S. A. Teukolsky, W. T. Vetterling, and B. P. Flannery, *Numerical Recipes* (Cambridge University Press, 1992).
 - [21] M. P. Hertzberg, R. L. Jaffe, M. Kardar, and A. Scardicchio, *Phys. Rev. Lett.* **95**, 250402 (2005).